OPEN ACCESS

University of BRISTOL

Aza, C., Pirrera, A., & Schenk, M. (2018). Reconfigurable Trusses of Nonlinear Morphing Elements. In *Proceedings of the ASME 2018 International Design Engineering Technical Conferences & Computers and Information in Engineering Conference (IDETC/CIE 2018)* [V05BT07A004] American Society of Mechanical Engineers (ASME). https://doi.org/10.1115/DETC2018-85911

Peer reviewed version

Link to published version (if available):
10.1115/DETC2018-85911

Link to publication record in Explore Bristol Research
PDF-document

This is the author accepted manuscript (AAM). The final published version (version of record) is available online via ASME at http://proceedings.asmedigitalcollection.asme.org/proceeding.aspx?articleid=2713496 . Please refer to any applicable terms of use of the publisher.

University of Bristol - Explore Bristol Research
General rights

This document is made available in accordance with publisher policies. Please cite only the published version using the reference above. Full terms of use are available:
http://www.bristol.ac.uk/red/research-policy/pure/user-guides/ebr-terms/

Proceedings of the ASME 2018 International Design Engineering Technical Conferences & Computers and Information in Engineering Conference
IDETC/CIE 2018
August 26-29, 2018, Quebec City, Quebec, Canada

DETC2018-85911

RECONFIGURABLE TRUSSES OF NONLINEAR MORPHING ELEMENTS

Chrysoula Aza
Bristol Composites Institute (ACCIS)
University of Bristol
Bristol, BS8 1TR, UK
E-mail: chrysoula.aza@bristol.ac.uk

Alberto Pirrera
Bristol Composites Institute (ACCIS)
University of Bristol
Bristol, BS8 1TR, UK
E-mail: alberto.pirrera@bristol.ac.uk

Mark Schenk
Bristol Composites Institute (ACCIS)
University of Bristol
Bristol, BS8 1TR, UK
E-mail: m.schenk@bristol.ac.uk

ABSTRACT

Reconfigurable mechanisms are capable of changing their behavior during operation and perform different tasks through changes of their configuration. A compliant, multistable, reconfigurable mechanism is introduced which consists of nonlinear morphing elements assembled in a truss-like configuration. These constituent elements are made of composite strips assembled to form a double-helix and exhibit tailorable nonlinear stiffness characteristics, including bistability. The mechanism's behavior can be tailored by tuning the inherent properties of the helical components, leading to a wide range of responses. This work explores the reconfigurability of the mechanism, based on the ability to change the helical pitch and the resulting stiffness.

INTRODUCTION

Over the past decades, the interest of researchers in reconfigurable mechanism has increased [1]. The capability of a mechanism to change its configuration, and to operate with different modes that can be exploited to serve multiple purposes, is what triggered the scientific interest in reconfigurable mechanisms [2]. Reconfigurability is attractive for numerous applications, such as antennas [3,4], deployable structures [5,6], robotics [7-9], or even in carton packaging manipulation [2], where there is a need for change in structural configuration and behavior for adaptation to different operating requirements.

Various ways to achieve reconfigurability have been investigated [1]. Most of the approaches developed focus on achieving reconfigurability through changes of the joint motion range [10], a mechanism's mobility or degrees of freedom [11,12], alterations in the geometry [13], orientation and number of links [14,15] or a combination of the above [16]. Controlling the mobility of revolute joints has been a common means to attain reconfiguration [6,7,12,13,16,17]. Alternative ways are based on the use of functional materials, such as shape memory alloys and the principles of origami [18].

In this paper, a compliant mechanism is proposed, which is able to change its behavior and operate in different modes, whilst maintaining its connectivity and mobility. Reconfigurability in this mechanism is achieved through the exploitation of the inherently nonlinear elastic characteristics of the constitutive elements, not the joint characteristics. The mechanism consists of morphing composite structures assembled in a truss-like configuration. Specifically, we use the composite structure of double-helix architecture developed by Lachenal *et al*. [19]. Its variable geometry and customizable nonlinear stiffness characteristics enable the mechanism to be tailored, and a variety of potential behaviors to be developed.

In the following sections, we first introduce the mechanism and its constituent morphing elements. The ensuing reconfigurability and stability characteristics are then explored using both an energy approach and a path-following method to trace the mechanism's response in force-displacement space. Conclusions are drawn in the last section.

Copyright © 2018 by ASME

TRUSSES OF NONLINEAR ELEMENTS

Double-Helix Element

The helical structure, used as the main component of the proposed mechanism, consists of two composite (carbon fibre reinforced plastic) strips of dimensions $L \times W$, connected by rigid spokes (Fig. 1). The spokes maintain the strips at a constant distance $H = 2R$, where R is the radius of an underlying cylinder, upon which the deformed strips can be assumed to lie [19,20]. Pre-stress is introduced in the strips by manufacturing them on a cylindrical mould of radius R_i and subsequently flattening them to form the double-helix. The double-helix is able to twist under the application of an axial force at its ends, which results in large axial displacements, Δl.

The structure can deform from a straight to a completely coiled configuration. The configuration is defined by the helix angle $\theta \in [-90°, 90°]$ between the local x-axis attached to each strip and the global X-axis [19,21]. Crucially, in the straight configuration ($\theta = 0°$), the structure can be nudged into one of two connected, but distinct, deformation modes: one with $\theta \in [0°, 90°]$ or one with $\theta \in [0°, -90°]$ (Fig. 1c, d). In addition, the structure features bistability, meaning that two self-equilibrated shapes, or in other words equilibria, exist; one per deformation mode.

The helical structure exhibits tailorable stiffness characteristics and strain energy profiles that can be customized by tuning various design parameters, such as the lay-up, pre-stress and geometry of the strips [13]. Lachenal *et al*. [19,21] developed an analytical model of the strain energy of the helix that can be expressed as:

$$U = \frac{n}{2}\int_0^L \int_{-W/2}^{W/2} \begin{bmatrix} \boldsymbol{\varepsilon}^0 \\ \Delta\boldsymbol{\kappa} \end{bmatrix}^{\mathrm{T}} \begin{bmatrix} \mathbf{A} & \mathbf{B} \\ \mathbf{B} & \mathbf{D} \end{bmatrix} \begin{bmatrix} \boldsymbol{\varepsilon}^0 \\ \Delta\boldsymbol{\kappa} \end{bmatrix} dxdy, \qquad (1)$$

where n is the number of strips constituting the structure and where, following Classical Laminate Theory [22], **A**, **B** and **D** are the in-plane, bending-extension coupling and bending stiffness matrices; $\boldsymbol{\varepsilon}^0$ is the vector of mid-plane strains—noting that uniform mid-plane deformations are assumed—and $\Delta\boldsymbol{\kappa}$ is the vector of changes in bending and twist curvature, with both vectors defined in the local coordinate system attached to each strip. The axial force necessary to deform the double-helix can be derived from the strain energy by application of Castigliano's theorem [19].

Figure 2 shows the evolution of the strain energy and the axial blocking force of the helix over its entire work space. Both quantities are shown as a function of θ and Δl, and for double-helices of different laminates of symmetric and antisymmetric stacking sequence: respectively, $[\beta_2/0/\beta_2]$ and $[\beta_2/0/-\beta_2]$, where $\beta \in [0°, 90°]$ is the fiber angle with respect to the longitudinal axis of the strip. For strips where $\beta = 0°$, $\beta = 90°$ or antisymmetric ones, the strain energy is periodic and symmetric with respect to $\theta = 0°$ (Fig. 2a), meaning that, in these cases, helices will exhibit identical behaviors in $\theta \in [0°, 90°]$ and $\theta \in [0°, -90°]$, and therefore, the same force-displacement response (single lines in Fig. 2b for these lay-ups). This is in contrast to the behavior of symmetric angle-ply lay-ups. For instance, the strain energy for the $[45_2/0/45_2]$ layup in Fig. 2 retains the periodicity, but breaks the symmetry around $\theta = 0°$, meaning that the force-displacement response will differ in $\theta \in [0°, 90°]$ and $\theta \in [0°, -90°]$ (two lines in Fig. 2b). Since this difference provides the basis for the reconfigurability of the

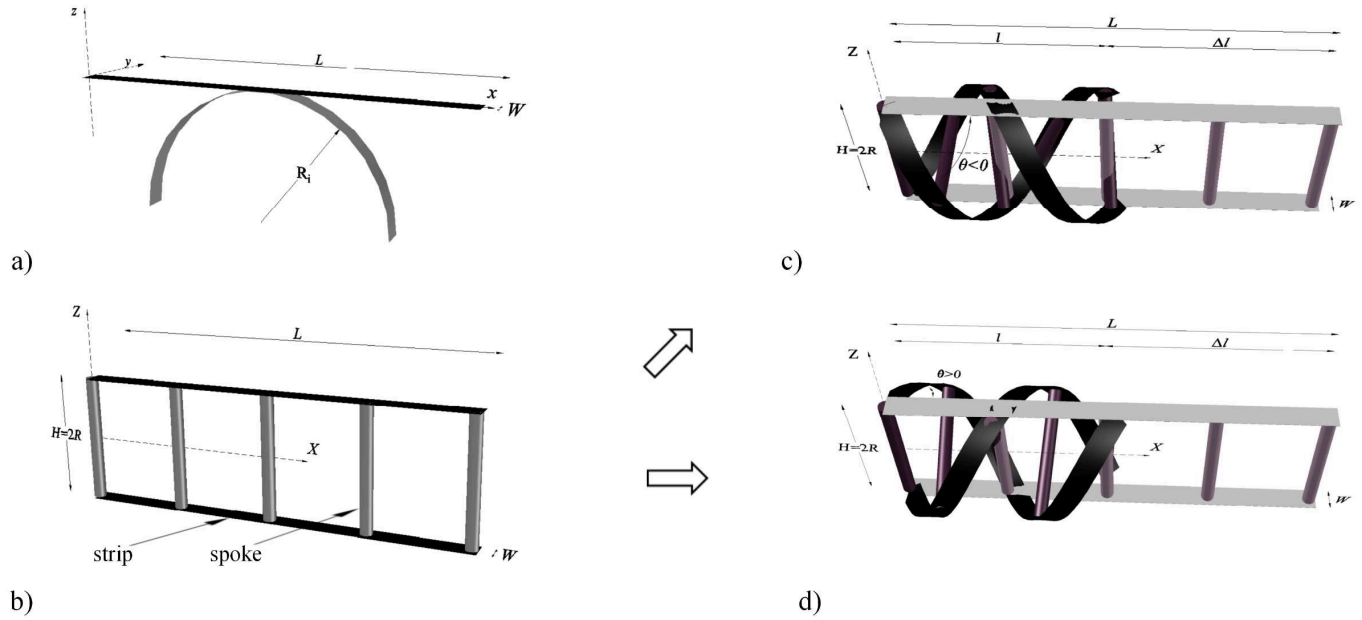

Figure 1. a) Flattening of the initially curved strips; b) double-helix geometry; Straight (light grey) and twisted (dark) configurations of the double-helix composite structure with (c) $\theta \in [0°, -90°]$ and (d) $\theta \in [0°, 90°]$.

Copyright © 2018 by ASME

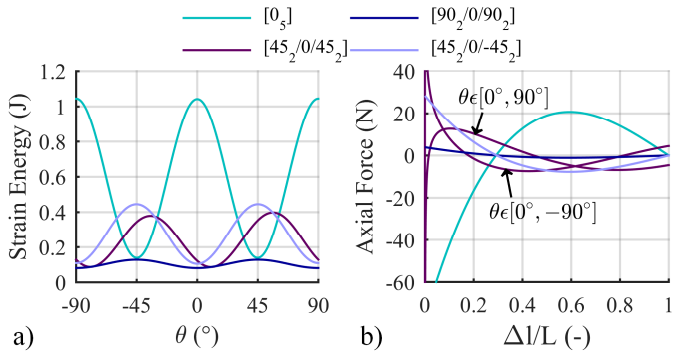

Figure 2. a) Strain energy profiles as a function of the helix angle θ and b) corresponding load-displacement curves of double-helices with $L = 95$ mm, $R = 15$ mm, $R_i = 30$ mm, $W = 5$ mm for different strip lay-ups. The displacement Δl is normalized to the length L of the strips.

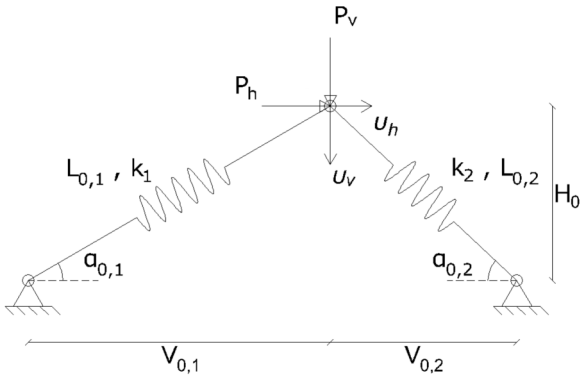

Figure 3. Schematic representation of the assembly of double-helices in a truss-like configuration.

helix, only symmetric lay-ups of the form $[\beta_2/0/\beta_2]$ are considered herein.

Assembly of the Mechanism

The mechanism studied herein is depicted in Fig. 3. It consists of two double-helical elements assembled in a truss configuration with pin joints at the apex and base supports. This configuration has been chosen as a balance between simplicity, generality and the ability to showcase and demonstrate reconfigurability.

The initial configuration of the mechanism has height H_0 and members of length $L_{0,i}$, with $i = 1, 2$. The double-helical elements have nonlinear axial stiffness k_i and form an angle $\alpha_{0,i}$ with the horizontal. Upon application of an external load, the apex is free to move horizontally and vertically by v_h, v_v, respectively. Note that the initial lengths $L_{0,i}$ (see Fig. 3) correspond to the dimension of the double-helices in their extended equilibrium position. In the first instance, the double-helices are set to coil with θ in the range [0°, 90°].

In the following, we shall assume for simplicity that the truss consists of two identical helices, which can be reconfigured individually by changing their twist orientation.

ANALYSIS

First, energy landscapes are employed to capture the mechanism's behavior and to identify stable and unstable regions over its work space. Stable and unstable equilibria are pinpointed, respectively, as minima and maxima of the strain energy functional. Next, a path-following method is used to investigate the response of the mechanism under a specific load case and to obtain potential load paths between stable positions.

Energy Approach

The stability of the mechanism is identified by inspection of its strain energy landscape. For the assembly of Fig. 3, the total strain energy is uniquely determined by the position of the end effector (the apex), and is the sum of the strain energy of the constituent helical members [23], calculated using Eq. (1).

Path-following Method

A path-following method, specifically the modified-Riks method developed by Crisfield [24], is employed for the analysis of the assembly in force-displacement space. The system of governing equilibrium equations is obtained by balancing the forces acting on the mechanisms (both internal and external) and deriving k_1 and k_2 by differentiation of Eq. (1) [19,24]. The nonlinear characteristics of the system and our interest in its snap-through and snap-back behavior, make path-following particularly suited [25,26]. Additionally, the eigenvalues of the system's tangential stiffness matrix are inspected to characterize the stability of points in the equilibrium loci—with negative eigenvalues indicating instability—but also to detect bifurcations, *i.e.* points of singularity of the tangent stiffness matrix. Branches originating thereof are then traced by perturbing the equilibria at the bifurcation points using the eigenvector corresponding to the null eigenvalue [27,28].

RESULTS AND DISCUSSION

The reconfigurability of the mechanism is explored by studying the behavior and stability characteristics of the truss-like assembly. The influence on the mechanism's behavior of the double-helices' design parameters, and of the initial geometry of the truss itself, is explored. First, we investigate steep trusses by analyzing the strain energy landscapes corresponding to all possible combinations of the helical deformation modes. We then study the trusses' response upon application of a vertical load at the end effector. Next, these results are compared to those for trusses with double-helices of different lay-ups, as well as to those for shallower trusses.

Reconfigurability

The stiffness properties of double-helices with symmetric lay-ups differ for pitch angles θ in [0°, 90°] or [0°, −90°] (Fig. 2). This allows the mechanism to be reconfigured to exhibit different responses. The mechanism can be reconfigured by forcing it onto a state where one or both helices are fully extended and then nudging either one or both to switch twisting mode. Three different mechanism modes can be obtained

Copyright © 2018 by ASME

combinatorically from the two helical modes. More specifically, the mechanism can be reconfigured into the following modes:

- **Mode I**: both helices twist with helix angle $\theta \in [0°, 90°]$;
- **Mode II**: both helices twist with helix angle $\theta \in [0°, -90°]$;
- **Mode III**: one helix deforms with $\theta \in [0°, 90°]$, and the second with $\theta \in [0°, -90°]$.

Figure 4 depicts the strain energy landscapes for the three potential reconfiguration modes for mechanisms consisting of double-helices of a $[45_2/0/45_2]$ lay-up, arranged in a steep configuration with $\alpha_{0,1} = 70°$. Stable and unstable equilibria, *i.e.* minima and maxima of the energy landscape, are marked, respectively, with Arabic numerals and letters. Additionally, stable equilibria may be found on the boundary of the landscape. These points are marked with Roman numerals. For Mode I (Fig. 4a), the mechanism displays quadristability; specifically, four interior minima. Conversely, Mode II (Fig. 4b) features only one interior minimum, plus four boundary equilibria. Mode III features ten extrema, of which two are minima, and three additional stable boundary equilibria.

The force-displacement response of the mechanism upon application of a vertical load at the end effector is presented in Fig. 5. The corresponding solution manifolds are superimposed on the strain energy plots in Fig. 4. For Mode I, a bifurcation is present, resulting in sideways apex displacements. Two of the

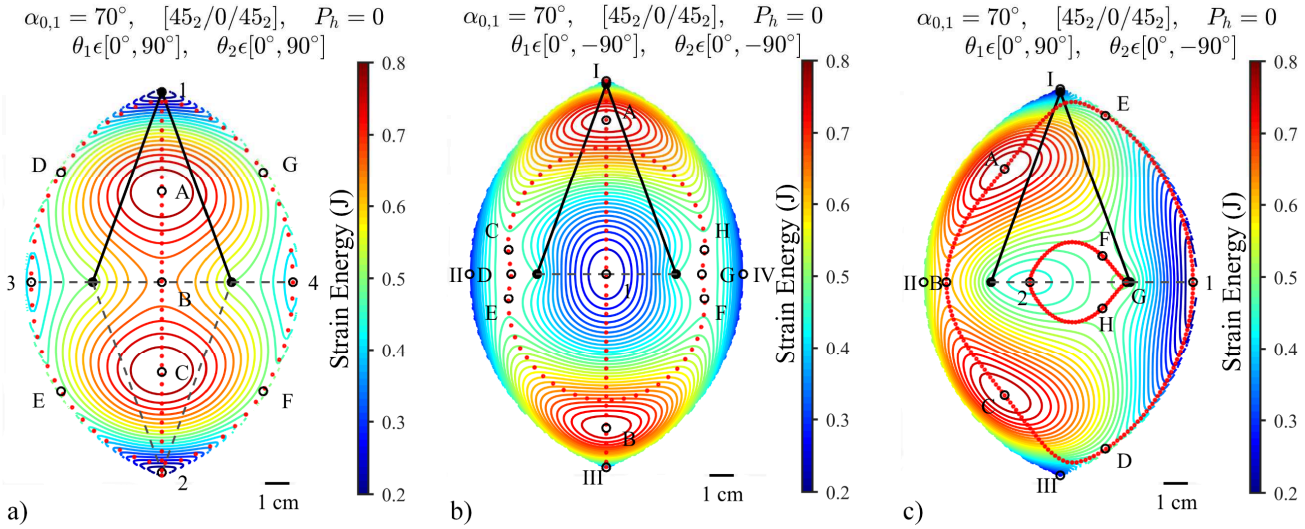

Figure 4. Strain energy landscapes for a compliant mechanism of double-helices of a $[45_2/0/45_2]$ composite strip lay-up, L = 95 mm, R = 15 mm, R_i = 30 mm, W = 5 mm assembled in a truss-like configuration with an initial angle $\alpha_{0,1} = 70°$ for different reconfiguration modes. a) Mode I: $\theta_i \in [0°, 90°]$; b) Mode II: $\theta_i \in [0°, -90°]$; c) Mode III: $\theta_1 \in [0°, 90°]$, $\theta_2 \in [0°, -90°]$. Points labelled 1–4 denote stable equilibria, while points A–H identify positions of unstable equilibrium. Points I-IV denote stable boundary equilibria. Red points indicate the equilibrium paths of the apex under the application of a vertical load ($P_h = 0$).

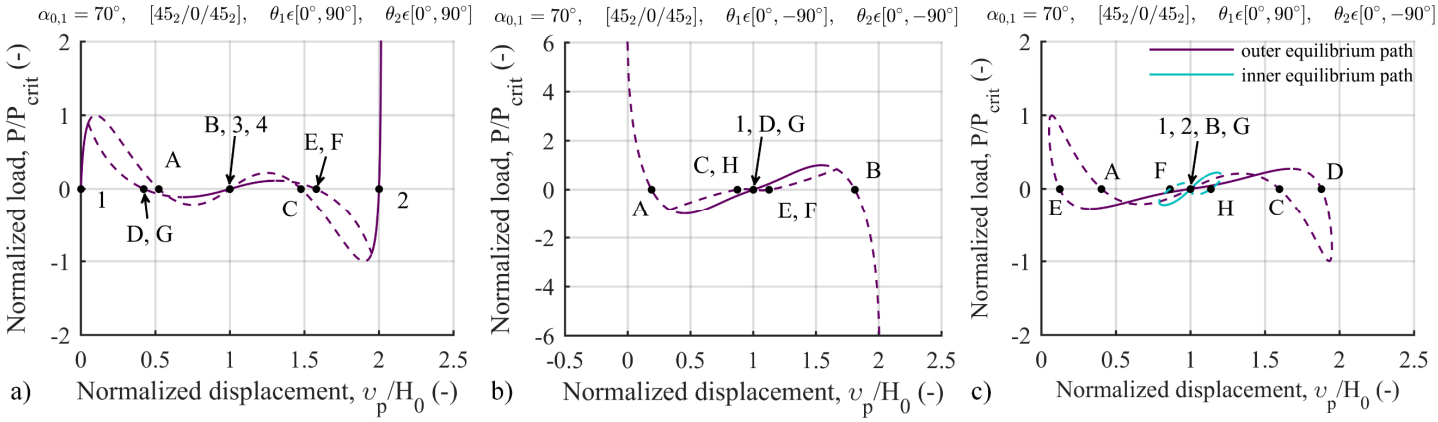

Figure 5. Load-displacement curves of the truss with an initial angles $\alpha_{0,1} = 70°$ for different reconfiguration modes consisting of double helices of $[45_2/0/45_2]$ layup, L = 95 mm, R = 15 mm, R_i = 30 mm, W = 5 mm under the application of a vertical load at the apex. Points 1–4 are stable equilibrium points. Point A–H are unstable equilibrium points. Dashed line represents the areas of instability. The load is normalized with respect to the load value at the maximum peak (P_{crit}) in each case.

Copyright © 2018 by ASME

four stable states are located on the main (vertical) path, *i.e.* the initial configuration and the fully inverted state at a vertical displacement of $2H_0$ (points 1 and 2, in Fig. 5a). The other two equilibria are on the bifurcated branch on the horizontal, *i.e.* at a vertical displacement of H_0 (points 3 and 4 in Fig. 5a). A bifurcation is present in Mode II as well, though the only stable interior configuration occurs when the double-helices are collinear with zero horizontal displacement of the apex (point 1 in Fig. 5b). Along the bifurcated path two areas of nearly zero force can be observed for the motion range between points C, D, E and F, G, H (Fig. 5b). In Mode III, no bifurcation occurs, however, the end effector experiences both horizontal and vertical displacement. Two independent closed loop equilibrium paths are identified with one stable equilibrium each. The stable states are encountered when the double-helices are collinear (points 1 and 2 in Fig. 5c).

Effect of Composite Lay-up

The composite lay-up affects the properties of the double-helices, namely their nonlinear axial stiffness, and thus the characteristics of the assembly. In this section, we investigate the effect of lay-up on the various reconfiguration modes.

Mode I. Figure 6 shows the energy landscapes for a truss identical to that of Fig. 4a, with the strips' lay-up changed to $[30_2/0/30_2]$ and $[60_2/0/60_2]$. The landscapes show no qualitative differences, apart from overall rescaling, and changes in the absolute values and relative positions of the extrema. In conclusion, all characteristic features, including quadristability,

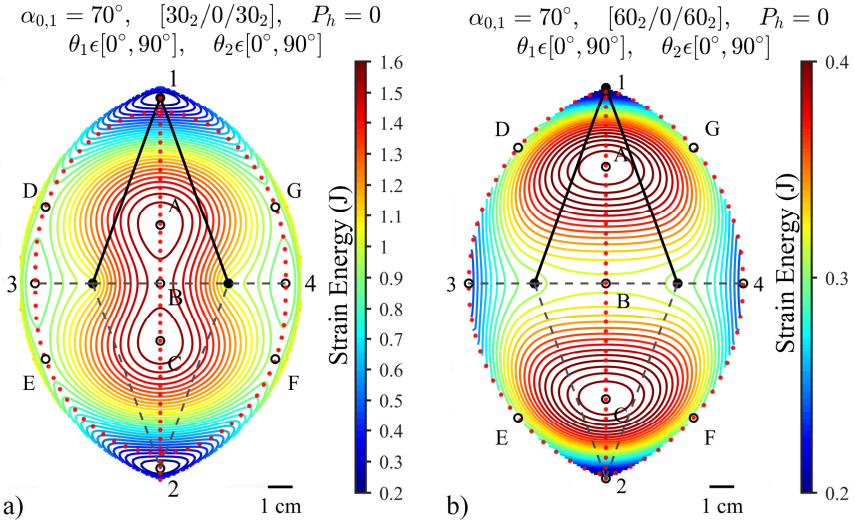

Figure 6. Strain energy landscapes for a compliant mechanism of double-helices of L = 95 mm, R = 15 mm, R_i = 30 mm, W = 5 mm assembled in a truss-like configuration with an initial angle $\alpha_{0,1}$ = 70° for composite strips of $[\beta_2/0/\beta_2]$ lay-up for the reconfiguration Mode I. a) $[30_2/0/30_2]$; b) $[60_2/0/60_2]$. Points labelled 1–4 denote stable equilibria, while points A–G identify positions of unstable equilibrium. Red points indicate the equilibrium paths of the apex under the application of a vertical load (P_h = 0).

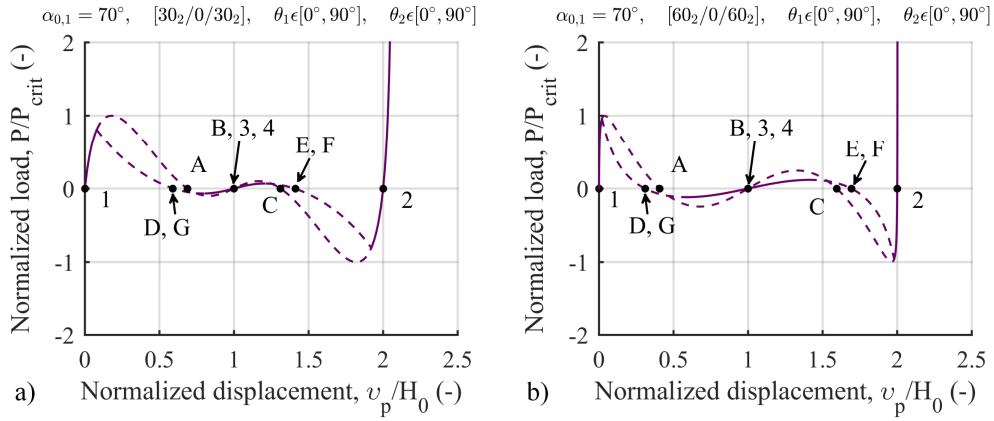

Figure 7. Load-displacement curves of the truss with an initial angles $\alpha_{0,1}$ = 70° for different lay-ups for the reconfiguration Mode I, under the application of a vertical load at the apex. a) $[30_2/0/30_2]$; b) $[60_2/0/60_2]$. Points 1–4 are stable equilibrium points. Point A–G are unstable equilibrium points. Dashed line represents the areas of instability. The load is normalized with respect to the load value at the maximum peak (P_{crit}) in each case.

Copyright © 2018 by ASME

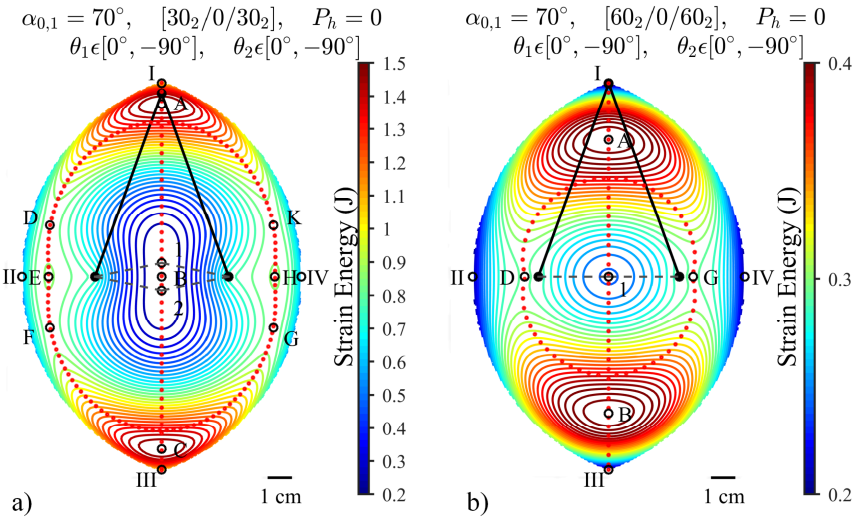

Figure 8. Strain energy landscapes for a compliant mechanism of double-helices of L = 95 mm, R = 15 mm, R_i = 30 mm, W = 5 mm assembled in a truss-like configuration with an initial angle $\alpha_{0,1}$ = 70° for composite strips of $[\beta_2/0/\beta_2]$ lay-up for reconfiguration Mode II. a) $[30_2/0/30_2]$; b) $[60_2/0/60_2]$. Points labelled 1 and 2 denote stable equilibria, while points A–H and K identify positions of unstable equilibrium. Points I-IV denote stable boundary equilibria. Red points indicate the equilibrium paths of the apex under the application of a vertical load (P_h = 0).

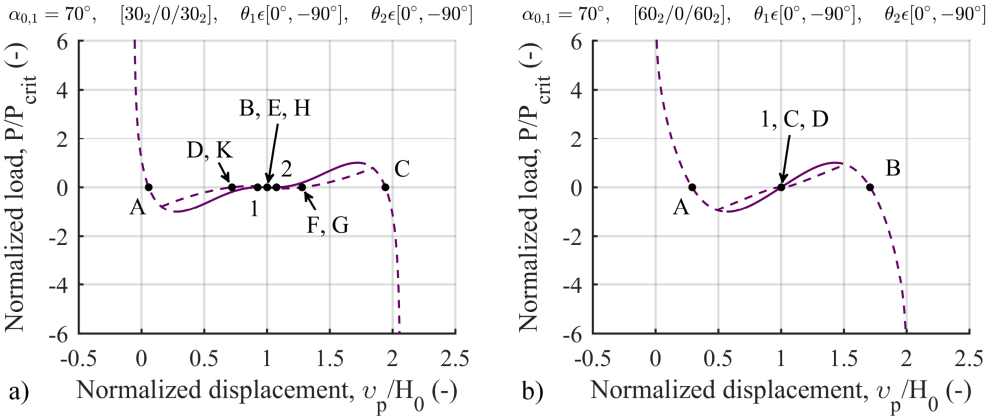

Figure 9. Load-displacement curves of the truss with an initial angles $\alpha_{0,1}$ = 70° for different lay-ups for the reconfiguration Mode II, under the application of a vertical load at the apex. a) $[30_2/0/30_2]$; b) $[60_2/0/60_2]$. Points 1 and 2 are stable equilibrium points. Point A–H and K are unstable equilibrium points. Dashed line represents the areas of instability. The load is normalized with respect to the load value at the maximum peak (P_{crit}) in each case.

bifurcations and the connectivity between stable equilibria, are preserved. Figure 7 shows the load-displacement curves corresponding to the two laminate lay-ups.

Mode II. Figure 8 shows the energy landscapes for a truss identical to that of Fig. 4b, with the strips' lay-up changed to $[30_2/0/30_2]$ and $[60_2/0/60_2]$, where the helices are now set for Mode II. For a $[30_2/0/30_2]$ lay-up the truss develops two interior stable equilibria (marked as points 1 and 2 in Fig. 8a), positioned slightly above and below the center of the landscape where the single minimum for the $[45_2/0/45_2]$ configuration is located. Again, apart from overall rescaling of the energy values and changes of the relative distance between extrema, all other features are maintained, leading to a total of eleven interior equilibrium configurations. Although shallower, the boundary equilibria too are maintained. As for the $[45_2/0/45_2]$ case, for $\beta = 60°$ the mechanism exhibits a single stable equilibrium configuration, when the double-helices are collinear and the apex horizontal displacement is zero (point 1 in Fig. 8b), as well as four boundary equilibria. The mechanism's force-displacement response upon application of a vertical load at the end effector is presented in Fig. 9, with the corresponding apex position superimposed once more on the strain energy plots (Fig. 8). The bifurcations are preserved for both the $[30_2/0/30_2]$ and the $[60_2/0/60_2]$ lay-ups; still none of the equilibrium positions on the bifurcated branch is stable. For $\beta = 30°$, areas of nearly zero force are present, both in the principal and bifurcated branch, for motion along the positions D, E and F, or 1, B and 2, or G, H and K (Fig. 9a). For $\beta = 60°$, the number of unstable equilibrium points along the bifurcated path reduced from six for the $[45_2/0/45_2]$ and $[30_2/0/30_2]$ lay-ups to two.

Copyright © 2018 by ASME

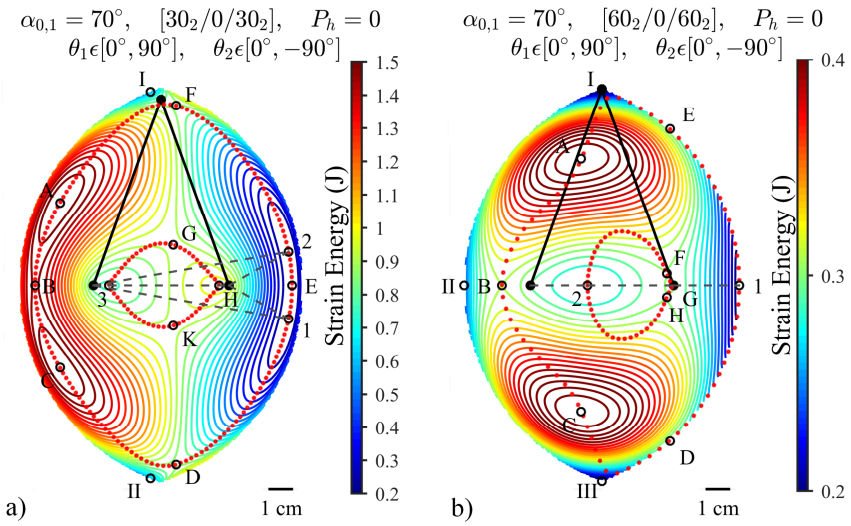

Figure 10. Strain energy landscapes for a compliant mechanism of double-helices of L = 95 mm, R = 15 mm, R_i = 30 mm, W = 5 mm assembled in a truss-like configuration with an initial angle $\alpha_{0,1}$ = 70° for composite strips of $[\beta_2/0/\beta_2]$ lay-up for reconfiguration Mode III. a) $[30_2/0/30_2]$; b) $[60_2/0/60_2]$. Points labelled 1–3 denote stable equilibria, while points A–H and K identify positions of unstable equilibrium. Points I-III denote stable boundary equilibria. Red points indicate the equilibrium paths of the apex under the application of a vertical load (P_h = 0).

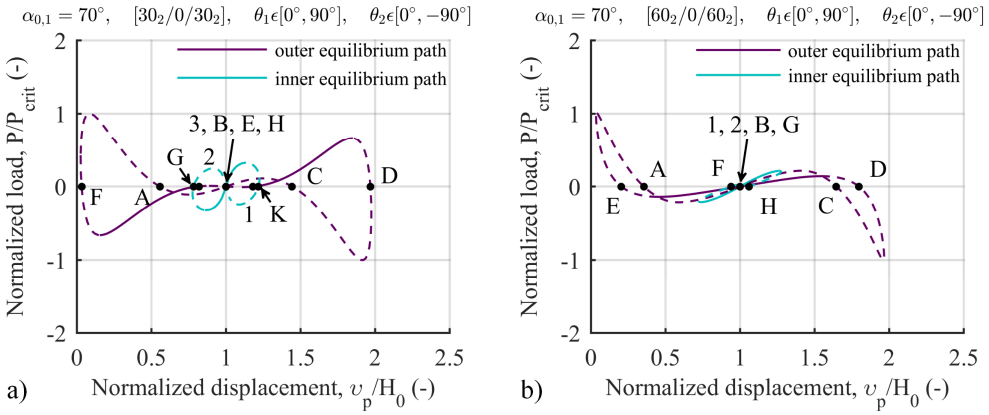

Figure 11. Load-displacement curves of the truss with an initial angles $\alpha_{0,1}$ = 70° for different lay-ups for the reconfiguration Mode III under the application of a vertical load at the apex. a) $[30_2/0/30_2]$; b) $[60_2/0/60_2]$. Points 1–3 are stable equilibrium points. Point A–H and K are unstable equilibrium points. Dashed line represents the areas of instability. The load is normalized with respect to the load value at the maximum peak (P_{crit}) in each case.

Mode III. The strain energy landscapes for Mode III are presented in Fig. 10. For $\beta = 30°$, a total of twelve interior equilibrium positions are identified, of which three are stable (marked as points 1–3 in Fig. 10a). The mechanism is bistable for a $[60_2/0/60_2]$ lay-up, with the two stable states when the two double-helices are collinear (points 1 and 2 in Fig. 10b). Figure 11 presents the load-displacement curves under a vertical load at the apex. The corresponding positions of the apex are superimposed on the strain energy plots in Fig. 10. Similarly to the $[45_2/0/45_2]$ lay-up, for both ply angles, two independent closed loop equilibrium paths are found, with the apex experiencing both horizontal and vertical displacement, and with stable equilibrium positions present in both paths (points 1–3 in Fig. 11). Though only for $\beta = 30°$, a nearly zero force area can be observed in the outer equilibrium path (motion range among points 1, E and 2 in Fig. 11a).

Effect of Initial Truss Angle

Finally, the effect of the initial truss geometry on the mechanism's behavior and its reconfigurability is explored. Figure 12 presents the strain energy landscapes for a shallow truss configuration with $\alpha_{0,1}$ = 35° and a $[45_2/0/45_2]$ strip lay-up for the three reconfiguration modes.

For a shallow truss with double-helices operating in Mode I, a total of five equilibrium positions are identified with only two being stable (marked as points 1 and 2 in Fig. 12a), compared to the four stable configurations out of a total of eleven equilibria in a steep truss (marked as points 1–4 in Fig. 4a). Mode II for a shallow truss shows three interior equilibrium positions,

Copyright © 2018 by ASME

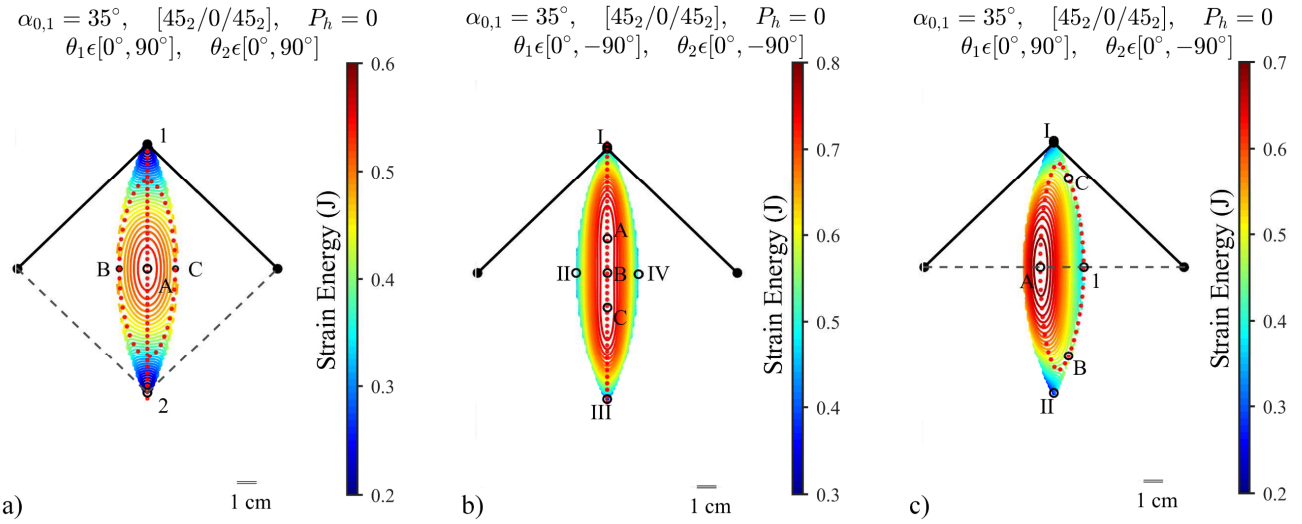

Figure 12. Strain energy landscapes for a compliant mechanism of double-helices of a [45₂/0/45₂] composite strip lay-up, L = 95 mm, R = 15 mm, R_i = 30 mm, W = 5 mm assembled in a truss-like configuration with an initial angle $\alpha_{0,1}$ = 35° for different reconfiguration modes. a) Mode I: $\theta_i \epsilon$ [0°, 90°]; b) Mode II: $\theta_i \epsilon$ [0°, −90°]; c) Mode III: $\theta_1 \epsilon$ [0°, 90°], $\theta_2 \epsilon$ [0°, −90°]. Points labelled 1 and 2 denote stable equilibria, while points A–C identify positions of unstable equilibrium. Points I-IV denote stable boundary equilibria. Red points indicate the equilibrium paths of the apex under the application of a vertical load (P_h = 0).

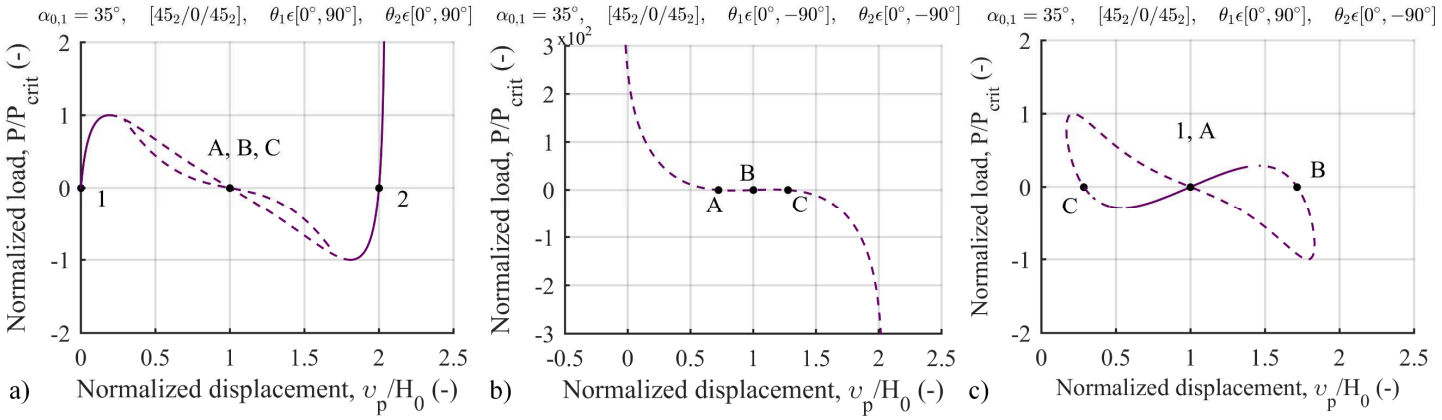

Figure 13. Load-displacement curves of the truss with an initial angles $\alpha_{0,1}$ = 35° for different reconfiguration modes consisting of double helices of [45₂/0/45₂] layup, the application of a vertical load at the apex. a) Mode I; b) Mode II; c) Mode III. Points 1 and 2 are stable equilibrium points. Point A–C are unstable equilibrium points. Dashed line represents the areas of instability. The load is normalized with respect to the load value at the maximum peak (P$_{crit}$) in each case.

none of which are stable (Fig. 12b), and four stable boundary equilibria (points I-IV). This contrasts with the steep truss, which has a single stable interior equilibrium position. Mode III shows four interior equilibria, of which one is stable (point 1 in Fig. 12c).

The load-displacement curves for the shallow truss under a vertical load at the end effector are presented in Fig. 13. The apex positions are superimposed on the strain energy plots in Fig. 12. For reconfiguration Mode I, for both the shallow and steep truss, a bifurcation of the equilibrium path occurs. However, the shallow truss only displays bistability, with stable states at the initial configuration and at a vertical displacement of $2H_0$ (points 1 and 2, in Fig. 13a). For Mode II, the mechanism is unstable for a shallow truss. A statically balanced area with nearly zero force can be observed between points A, B and C (Fig. 13b). In this mode, no bifurcation occurs in the shallow truss, unlike in the steep truss, with the apex experiencing only a vertical displacement under the applied load. Mode III shows a closed loop load-displacement curve (Fig. 13c). The compliant mechanism displays monostability with the single stable point encountered in one of the configurations where the helices are collinear (point 1 in Fig. 12c). The mechanism experiences a single closed loop equilibrium path, as opposed to the behavior for a steep truss, where a second, disconnected equilibrium path is observed.

Copyright © 2018 by ASME

CONCLUSIONS

A reconfigurable, multistable mechanism consisting of morphing elements of a double-helix architecture arranged in a truss-like configuration has been introduced. The reconfigurability of the mechanism is based on the inherent ability of the double-helical elements to switch their twist direction when in the fully extended state. As a result, a mechanism with two identical double-helix elements can achieve three different reconfiguration modes (Mode I, Mode II and Mode III). The mechanism's multistability characteristics and its response in the force-displacement space are explored for the different reconfiguration modes.

Strain energy landscapes are used to identify stable and unstable equilibria, corresponding to valleys and peaks, respectively. A path-following method has been employed to trace equilibrium paths in force-displacement space for an applied vertical load at the apex.

It was shown that the reconfiguration modes significantly change the mechanical behavior of the mechanism studied. For a steep truss ($\alpha_{0,1} = 70°$) with a symmetric composite lay-up [$\beta_2/0/\beta_2$], the mechanism is quadristable in Mode I, and the equilibrium path bifurcates to access all equilibria. For Mode II, the response depends on the fiber angle, with $\beta = 30°$ showing bistability, and monostability for $\beta = 45°$ and $\beta = 60°$. Again, bifurcations of the equilibrium path enable all internal equilibria to be traversed under an applied vertical load. In Mode III, however, two disconnected equilibrium paths are identified, and the structure is bistable for $\beta = 45°$ and $\beta = 60°$, but tristable for $\beta = 30°$. The energy landscapes were found to be an effective means to convey the qualitative changes in mechanical behavior between the reconfiguration modes.

Future work will concentrate on the manufacturability of a prototype of this reconfigurable mechanism.

ACKNOWLEDGMENTS

This work was supported by the Engineering and Physical Sciences Research Council through the EPSRC Centre for Doctoral Training in Advanced Composites for Innovation and Science [grant number EP/L016028/1] and through the EPSRC Fellowship titled *Structural Efficiency and Multi-Functionality of Well-Behaved Nonlinear Composite Structures* [grant number EP/M013170/1].

REFERENCES

[1] Aimedee, Marie Fidele, Gogu, Grigore, Dai, Jian S, Bouzgarrou Belhassen Chedli and Bouton Nicolas. "Systematization of Morphing in Reconfigurable Mechanisms." *Mechanism and Machine Theory* Vol. 96 (2016): pp. 215-224. DOI: 10.1016/j.mechmachtheory.2015.07.009.

[2] Kuo, Chin-Hsing, Dai, Jian S and Yan, Hong-Sen. "Reconfiguration Principles and Strategies for Reconfigurable Mechanisms." *ASME/IFToMM International Conference on Reconfigurable Mechanisms and Robots.* pp. 1-7, London, UK, June 22-24, 2009.

[3] Ji, Lu-Yang, Guo, Yingjie Jay, Qin, Pei-Yuan, Gong, Shu-Xi and Mittra, Raj. "A Reconfigurable Partially Reflective Surface (PRS) Antenna for Beam Steering." *IEEE Transactions on Antennas and Propagation* Vol. 63 No. 6 (2015): pp. 2387-2395. DOI: 10.1109/TAP.2015.2412143.

[4] Guo, Yingjie Jay, Qin, Pei-Yuan, Chen, Shu-Lin, Lin, Wei and Ziolkowski, Richard W. "Advances in Reconfigurable Antenna Systems Facilitated by Innovative Technologies." *IEEE Access* Vol. 6 (2018): pp. 5780-5794. DOI: 10.1109/ACCESS.2017.2789199.

[5] Miura, Koryo. "Method of Packaging and Deployment of Large Membranes in Space." *The Institute of Space and Astronautical Science Report* Vol. 618 (1985): pp. 1-9. DOI: 10.1177/0096340215581359.

[6] Zhao, Jingshan, Yan, Zhengfang and Chu, Fulei. "A Reconfigurable Linkage and Its Application in Lift Mechanism." *2nd ASME/IFToMM International Conference on Reconfigurable Mechanisms and Robots* pp. 815–829, Tianjin, China; July 9-11, 2012. DOI: 10.1007/978-1-4471-4141-9_73.

[7] Wang, Wei, Zhang, Houxiang, Zong, Guanghua and Zhang, Jianwei. "Design and Realization of a Novel Reconfigurable Robot with Serial and Parallel Mechanisms." *Proceedings of IEEE International Conference on Robotics and, Biomimetics* pp. 697–702, Kunming, China, December 17-20, 2006. DOI: 10.1109/ROBIO.2006.340291.

[8] Wei, Guowu, Dai, Jian S, Wang, Shuxin and Luo, Haifeng. "Kinematic Analysis and Prototype of a Metamorphic Anthropomorphic Hand with a Reconfigurable Palm." *International Journal of Humanoid Robotics* Vol. 8 No. 3 (2011): pp. 459-479. DOI: 10.1142/S0219843611002538.

[9] Heidari, Hamidreza, Pouria, Milad Jafary, Sharifi, Shahriar and Karami, Mahmoudreza. "Design and Fabrication of Roboric Gripper for Grasping in Minimizing Contact Force." *Advances in Space Research* Vol. 61 (2018): pp.1359-1370. DOI: 10.1016/j.asr.2017.12.024.

[10] Zhang, Wuxiang, Ding, Xilun and Dai, Jian S. "Morphological Synthesis of Metamorphic Mechanisms Based on Constraint Variation." *Proceedings of the Institution of Mechanical Engineers, Part C: Journal of Mechanical Engineering Science* Vol. 225 No. 12 (2011): pp. 2297-2310. DOI: 10.1177/0954406211408953.

[11] Plitea, Nicoale, Lese, Dorin, Pisla, Doina and Vaida, Calin. "Structural Design and Kinematics of a New Parallel Reconfigurable Robot." *Robotics and Computer-Integrated Manufacturing* Vol. 29 (2013): pp. 219-235. DOI: 10.1016/j.rcim.2012.06.001.

[12] Galletti, Carlo and Fanghella, Pietro. "Single-Loop Kinematotropic Mechanisms." *Mechanism and Machine Theory* Vol. 36 No. 6 (2001): pp. 743-761. DOI: 10.1016/S0094-114X(01)00002-7.

[13] Dai, Jian S and Rees Jones, John. "Kinematics and Mobility Analysis of Origami-Carton Folds in Packing Manipulation Based on the Mechanism Equivalent." *Proceedings of the Institution of Mechanical Engineers, Part C: Journal of Mechanical Engineering Science* Vol. 216 No. 10 (2002): pp. 959-970. DOI: 10.1243/095440602760400931.

[14] Zhang, Liping and Dai, Jian S. "Reconfiguration of Spatial Metamorphic Mechanisms." *Journal of Mechanisms and*

 Copyright © 2018 by ASME

Robotics Vol. 1 No. 1 (2008): pp. 011012-1-011012-8. DOI: 10.1115/1.2963025.

[15] Leonesio, Marco, Bianchi, Giacomo and Manara, P. "A General Approach for Self-Locking Analysis in Closed Kinematic Chains." *Proceedings of the 12th World Congress in Mechanism and Machine Theory*. pp. 141–147, Besancon, France, June 18-21, 2007. DOI: 10.1016/j.mechmachtheory.2009.05.005.

[16] Li, Shujun and Dai, Jian S. "Structure Synthesis of Single-Driven Metamorphic Mechanisms Based on Augmented Assur Groups." *Journal of Mechanisms and Robotics* Vol. 4 No. 3 (2012): pp. 031004-1-031004-8. DOI: 10.1115/1.4006741.

[17] Gan, Dongming, Dai, Jian S and Liao, Qizheng. "Mobility Change in Two Types of Metamorphic Parallel Mechanisms." *Journal of Mechanisms and Robotics* Vol. 1 No. 4 (2009): pp. 041007-1-041007-9. DOI: 10.1115/1.3211023.

[18] Peraza Hernandez, Edwin A, Hartl, Darren J, Malak Jr, Richard J, Akleman, Ergun, Gonen, Ozgur and Kung Han-Wei. "Design Tools for Patterned Self-Folding Reconfigurable Structures Based on Programmable Active Laminates." *Journal of Mechanisms and Robotics* Vol.8 (2016): pp.031015-1-031015-12. DOI: 10.1115/1.4031955.

[19] Lachenal, Xavier, Weaver, Paul M and Daynes, Stephen. "Multi-stable Composite Twisting Structure for Morphing Applications." *Proceedings of the Royal Society A: Mathematical, Physical and Engineering Sciences* Vol. 468 No. 2141 (2012): pp. 1230-1251. DOI: 10.1098/rspa.2011.0631.

[20] Cappello, Leonardo, Lachenal, Xavier, Pirrera, Alberto, Mattioni, Filippo, Weaver, Paul M and Masia, Lorenzo. "Design, Characterization and Stability Test of a Multistable Composite Compliant Actuator for Exoskeletons." *5th IEEE RAS/EMBS International Conference on Biomedical Robotics and Biomechatronics*. pp. 1051-1056, Sao Paulo, Brazil, August 12-15, 2014. DOI: 10.1109/BIOROB.2014.6913919.

[21] Lachenal, Xavier, Weaver, Paul M and Daynes, Stephen. "Influence of Transverse Curvature on the Stability of Pre-Stressed Helical Structures." *International Journal of Solids and Structures* Vol. 51 No. 13 (2014): pp. 2479-2490. DOI: 10.1016/j.ijsolstr.2014.03.014.

[22] Kollar, Laszlo Peter and Springer, George S. *Mechanics of Composite Structures*. Cambridge University Press, Cambridge, UK (2003).

[23] Radaelli, Guiseppe, Gallego, Juan A and Herder Just L. "An Energy Approach to Static Balancing of Systems with Torsion Stiffness." *Journal of Mechanical Design* Vol. 133 (2011): pp. 091006-1-091006-8. DOI: 10.1115/1.4004704.

[24] Reddy, Junuthula Narasimha. *An Introduction to Nonlinear Finite Element Analysis: with Applications to Heat Transfer, Fluid Mechanics, and Solid Mechanics*. 2nd Ed, Oxford University Press, Oxford, UK (2015).

[25] Han, Jeong Sam, Muller, Claas, Wallrabe, Ulrike and Korvink, Jan G. "Design, Simulation, and Fabrication of a Quadstable Monolithic Mechanism with X- and Y- Directional Bistable Curved Beams." *Journal of Mechanical Design* Vol. 129 No. 11 (2007): pp. 1198-1203. DOI: 10.1115/1.2771577.

[26] Crisfield, Michael A. "A Fast Incremental/Iterative Solution Procedure That Handles "Snap-Through"." *Computers and Structures* Vol. 13 (1981): pp. 55-62. DOI: 10.1016/0045-7949(81)90108-5.

[27] Wagner, Werner and Wriggers, Peter. "A Simple Method for the Calculation of Postcritical Branches." *Engineering Computations* Vol. 5 (1988): pp. 103-109. DOI: 10.1108/eb023727.

[28] Wriggers, Peter and Simo, Juan C. "A General Procedure for the Direct Computation of Turning and Bifurcation Points." *International Journal for Numerical Methods in Engineering* Vol. 30 (1990): pp. 155-176, 1990. DOI: 10.1002/nme.16203001

 Copyright © 2018 by ASME